Maxwell, J. C., *A Treatise on Electricity and Magnetism*, V. I, 3rd Ed., Clarendon Press, Oxford (1892).
Neira, M. A., and A. C. Payatakes, "Collocation Solution of Creeping Newtonian Flow Through Sinusoidal Tubes," *AIChE J.*, **25**, 725 (1979).
Payatakes, A. C., Chi Tien, and M. R. Turian, "A New Model for Granular Porous Media. 1: Model Formulation," *AIChE J.*, **19**, 58 (1973).
——, "Trajectory Calculation of Particle Deposition in Deep Bed Filtration. 1: Model Formulation," *AIChE J.*, **20**, 889 (1974).
Saffman, P. G., "Dispersion Due to Molecular Diffusion and Macroscopic Mixing in Flow Through a Network of Capillaries," *J. Fluid Mech.*, **7**, 194 (1960).
Snyder, L. J., and W. E. Stewart, "Velocity and Pressure Profiles for Newtonian Creeping Flow in Regular Packed Beds of Spheres," *AIChE J.*, **12**, 167 (1966).
Sorensen, J. P., and W. E. Stewart, "Computation of Forced Convection in Slow Flow through Ducts and Packed Beds. II: Velocity Profile in a Simple Cubic Array of Spheres," *Chem. Eng. Sci.*, **29**, 819 (1974).
Taylor, G. I., "The Dispersion of Soluble Matter in Solvent Flowing Slowly Through a Tube," *Proc. Roy. Soc.*, **219**, 186, London (1953).
Wen, C. Y., and L. T. Fan, *Models for Flow Systems and Chemical Reactors*, Marcel Dekker, Inc., New York (1975).
Zick, A. A., and G. M. Homsy, "Stokes Flow through Periodic Arrays of Spheres," *J. Fluid Mech.*, **115**, 13 (1982).

Manuscript received January 26, 1983; revision received December 6, 1983, and accepted December 8.

A Heat Transfer Model for Tubes Immersed in Gas Fluidized Beds

A model for local heat transfer between a gas-fluidized bed and a submerged tube is proposed based on combined dense-phase and lean-phase transport. The heat transfer process during dense-phase contact at the tube surface is modeled by packet renewal mechanism and the transfer process during lean-phase contact by fluid convection mechanism. The model predictions show good agreement with experimental local and average heat transfer coefficient data for horizontal tubes.

R. CHANDRAN
Department of Mechanical Engineering
Ohio University
Athens, OH 45701
and
J. C. CHEN
Department of Chemical Engineering
Lehigh University
Bethlehem, PA 18015

SCOPE

Many applications of fluidized beds involve heat transfer to or from immersed tubes and tube bundles. The rate of heat transfer between a fluidized bed and a submerged tube depends upon a number of factors, including the properties of the bed material and the contact fluid, bed and tube geometries, and the fluidization state. Measurements of heat transfer between fluidized beds and immersed tubes have been carried out by many investigators and both experimental data and correlations are reported in the literature. Reviews of the work are given by Gelperin and Einstein (1971), Gutfinger and Abuaf (1974), Zabrodsky et al. (1976), and Saxena et al. (1978). Comparisons of design correlations for bed-to-tube heat transfer coefficient are presented in Ainshtein and Gelperin (1966), Chen (1976), Grewal and Saxena (1980, 1981), and Botterill et al. (1981). However, from an application standpoint, there still is a need for improved phenomenological understanding of the mechanisms and appropriate modeling of the transport processes.

The foregoing remarks are especially true for tubes placed horizontally in fluidized beds. Since the fluid flow is in a direction normal to the tube axis for horizontal tubes, it is incorrect to assume axial symmetry. Local heat transfer coefficients could, and indeed do, vary with circumferential position on the tube surface. A few studies (Gelperin et al., 1966; Berg and Baskakov, 1974; Chandran et al., 1980) have reported local measurements around horizontal tubes. However, correlations for local heat transfer coefficient do not seem to have been published to date.

The objective of this study was to develop a mechanistic model for the prediction of local heat transfer coefficients, using information on bed-surface contact dynamics from fluid mechanics investigations (Chandran and Chen, 1982).

CONCLUSIONS AND SIGNIFICANCE

The local heat transfer coefficient at the tube surface was expressed as a weighted average of the dense-phase and the lean-phase transfer coefficients. For the case of negligible radiant contribution, heat transfer during dense-phase contact was attributed to the surface renewal mechanism and was modeled as a transient conduction process. Heat transfer during lean-phase contact was postulated to occur by the fluid convection mechanism with attendant enhancement due to the presence of particles in the medium.

With input data on local fluidization parameters, the model was able to successfully predict both local and average heat transfer coefficients for a wide range of test conditions.

Correspondence concerning this paper should be addressed to R. Chandran.

The dense-phase contribution was found to be significant at low gas flow rates and for small particles. The lean-phase contribution became more important at high gas flow rates, for large particles, and for elevated pressure operation. The dense-phase and the lean-phase transport coefficients were observed to change both in magnitude and in their relative importance to predict the correct variation in the local heat transfer coefficient with test parameters.

BACKGROUND

A number of researchers have used the mechanistic approach (Saxena and Gabor, 1981) and have arrived at semiempirical relations for the heat transfer coefficient. The models that have been proposed, in cases where the contribution due to radiation is insignificant, are:

1. Film Model. A fluid film adjacent to the exchange surface constitutes the principal resistance to heat transfer and moving solid particles scour away the limiting film, reduce the resistance, and increase heat transfer. These models are based on the fluid convection mechanism and generally involve a steady-state concept of the heat transfer process. This hypothesis is not supported by the experiments of van Heerden et al. (1953) or Ziegler and Brazelton (1964).

2. Penetration Model. Either "packets" (Mickley and Fairbanks, 1955; Mickley et al., 1961) or "single" particles (Botterill and Williams, 1963; Ziegler et al., 1964) contact the heat exchange surface for a certain duration, are periodically replaced by fresh material, undergo transient conduction during the residence time at the surface, and thus serve to transfer heat by transport of sensible heat. These models utilize an unsteady state approach and are based on the "surface renewal" concept that accounts for particle convective transport.

The packet model, proposed by Mickley and Fairbanks (1955) treats the fluid-solid medium (packet) that comes into contact with the exchange surface as homogeneous and assigns it the average thermal properties of the bed at incipient fluidization. This is unrealistic since the effect of the transfer surface on local particle packing is ignored. The error introduced is likely to be significant, especially for short contact times.

Modifications have been suggested by different workers to improve the basic packet model cited above. Baskakov (1964) introduced an empirical, time-independent contact resistance at the wall-packet interface to achieve a good comparison with data. Yoshida et al. (1969) used an approach analogous to the film-penetration theory advanced by Toor and Marchello (1958) for gas absorption into liquids. The inclusion of a characteristic length that is usually unknown, and the retention of the low Fourier number deficiency of the original packet model were the limitations of this work. Koppel et al. (1970) not only invoked the film-penetration mechanism of Toor and Marchello to assign a finite thickness to the packet, but also allowed a nonzero surface-packet thermal resistance, in the manner of Baskakov (1964). Gelperin and Einstein (1971) solved the basic packet model in terms of two heat transfer resistances, one due to the increased voidage in the vicinity of the wall that extended to one-half the diameter of a particle, and the other due to an adjoining two-phase packet. Antonishin et al. (1974) analyzed heat conduction in a dispersed system by allowing for local temperature relaxation in the heterogeneous medium. Kubie and Broughton (1975) introduced the concept of a property boundary layer to account for the wall effect. Ozkaynak and Chen (1980) used the concept of penetration depth to make an allowance for the influence of the wall on packing at short residence times.

The single-particle model, proposed by Botterill and Williams (1963), recognized the heterogeneity of the fluidized media and considered transient conduction between the exchange surface and a contacting spherical particle immersed in fluid. The resulting parabolic differential equations were solved by a numerical scheme. This model turned out to be inappropriate for long residence times wherein the depth of heat penetration exceeded one particle diameter. Realization of this limitation led to the development of a two-particle model by Botterill and Butt (1968) and subsequently, a model based on a solid chain of unlimited length by Gabor (1970). All these models had to resort to an artificial fluid-film gap between the surface and the first row of particles to obtain a good data fit.

Ziegler et al. (1964) considered the unsteady-state heat absorption by a cold sphere immersed in stagnant gas and in contact with a hot wall. They solved for the time-mean heat transfer coefficient by using a gamma distribution for the residence time of the particles. This model resembles that of Botterill and Williams (1963) and suffers from similar limitations.

Some additional studies (Baskakov et al., 1973; Selzer and Thomson, 1977; Krause and Peters, 1979; Bock and Molerus, 1980) have provided comparisons of experimental heat transfer coefficient data with the predictions of selected penetration models.

3. Gas Convection. Many investigators (Zabrodsky, 1966; Botterill and Desai, 1972; Baskakov and Suprun, 1972; Denloye and Botterill, 1978; Canada and McLaughlin, 1978; Adams and Welty, 1979; Glicksman and Decker, 1980; Catipovic et al., 1980, 1982; Zabrodsky et al., 1981) have stressed the importance of gas-convective heat transfer for fluidization of large particles and elevated pressure operation, and have presented data, models, and correlations.

4. Turbulent Flow Model. Staub (1979) has proposed a turbulent gas-solids flow model to predict the heat transfer coefficients for tube banks immersed in fluidized beds. It is essentially intended for use under conditions of high gas flow velocity and large particle fluidization.

In order to determine the applicability of the mechanisms outlined above, it is necessary to know the transient contact characteristics between the bed emulsion and the heat transfer surface on a local basis. Until recently, a lack of such knowledge seriously hampered the development and use of phenomenological models. To date, only a few measurements of contact dynamics have been reported (Ozkaynak and Chen, 1978; Chandran and Chen, 1982).

MODEL

Formulation

It was apparent from capacitance probe measurements (Chandran and Chen, 1982) that the surface could experience alternating contact with a dense emulsion phase and a lean void phase. The criterion for demarcation between the dense and the lean phases is somewhat arbitrary, but the dense phase is envisaged as a fairly close-packed matrix of solid particles ($\alpha_D \sim 0.4$ to 0.8) and the lean phase is regarded as a gaseous medium with some entrained particles ($\alpha_L \sim 0.8$ to 1.0). The local heat flux at the tube surface can be cast in the form

$$q = q_L + q_D \tag{1}$$

The local heat transfer coefficient h can then be expressed as a weighted average of the dense and the lean phase transfer coefficients,

$$h = f_L h_L + (1 - f_L) h_D \tag{2}$$

Here f_L denotes fractional contact time of the lean phase.

It is now necessary to derive relations for the transport coefficients in each phase. It is suggested that lean-phase heat transfer

occurs primarily by fluid convection and dense-phase heat transfer by transient conduction due to the surface renewal process. Herein the case considered is one in which the contribution due to radiation is negligible.

Dense-Phase Heat Transfer

When dense-phase contact of the renewal type occurs at the exchange surface, heat is transferred by unsteady state conduction. However, for very long residence times the process becomes one of steady state; the fluid flowing through the interstices between particles acts as the transfer medium and finite heat transfer results due to the ventilation effect. It is now postulated that the effective heat transfer coefficient in the dense phase (h_D) can be expressed in terms of two components, one due to surface renewal of a medium with stagnant fluid (h_s) and the other due to fluid flow (h_f):

$$h_D = h_s + h_f \tag{3}$$

The unsteady-state component (h_s) can be evaluated by analyzing transient conduction into packed media. We have carried out such an analysis and have obtained numerical solutions (Chandran and Chen, 1985). These solutions, however, are not in a readily usable form for design purposes. Hence we have modified the packet theory limit solution to get the following closed-form relation for the surface renewal component:

$$h_s = 2C\sqrt{\frac{k_D C_{pD}}{\pi \bar{\theta}_D}} \tag{4}$$

This expression applies for the case of a constant wall temperature boundary condition. But, in practice, the physical condition lies between constant wall heat flux and constant wall temperature, especially for low thermal capacity heaters. The parameter $\bar{\theta}_D$ is the root-square-average residence time of the dense-phase packets. Over I occurrences of dense-phase contact (I packets), each with a different residence time of θ_{D_i}, the root-square-average residence time for constant wall temperature boundary condition is defined as

$$\bar{\theta}_D \equiv \left[\frac{\sum_{i=1}^{I} \theta_{D_i}}{\sum_{i=1}^{I} \sqrt{\theta_{D_i}}}\right]^2 \tag{5}$$

It has been shown by Ozkaynak and Chen (1978, 1980) that the above root-square-average is the correct mean to use for the effective residence time. Equations for h_s and $\bar{\theta}_D$ that apply to constant wall heat flux boundary condition are given in the Appendix.

C in Eq. 4 is an effective correction factor that modifies the packet theory limit solution. It has been determined by matching the modified solution with the numerical solution, and is given by

$$C = \exp\left[-\frac{a_1}{Fo^{a_2 + a_3 \ln Fo}}\right] \tag{6}$$

with

$$a_1 = 0.213 + 0.117w + 0.041w^2$$
$$a_2 = 0.398 - 0.049w$$
$$a_3 = 0.022 - 0.003w$$
$$w = \ln(k_D/k_g)$$
$$Fo = k_D\bar{\theta}_D/C_{pD}\bar{d}_p^2$$

The physical properties (k_D, C_{pD}) are assigned the "bulk" values for the dense phase:

$$k_D = k^o$$
$$C_{pD} = \rho_s(1 - \alpha_D)c_{ps} + \rho_g\alpha_D c_{pg} \tag{7}$$

There exist several models for the determination of k^o (Kunii and Smith, 1960; Kunii and Yagi, 1960; Gelperin and Einstein, 1971; Bauer and Schlunder, 1978). The method proposed by Bauer and Schlunder (1978) has been selected for use in this study, due to its versatility and its completeness. In addition to the particle and fluid thermal properties, it accounts for the influence of temperature, pressure, particle shape, size-distribution and porosity, oxide layer, and finite contact surface area on the thermal conductivity of the two-phase medium. For closely-sized spherical particles and for operation at room temperature and gas pressure of 1 atmosphere (101.3 kPa) or above, the thermal conductivity of the medium could be estimated from

$$k^o = k_g\left[(1 - \sqrt{1 - \alpha_D}) + \sqrt{1 - \alpha_D}\left(\frac{k'}{k_g}\right)\right] \tag{8}$$

with

$$\frac{k'}{k_g} = \frac{2}{\left(1 - B\frac{k_g}{k_s}\right)}\left[\frac{\left(1 - \frac{k_g}{k_s}\right)B}{\left(1 - B\frac{k_g}{k_s}\right)^2}\ln\left(\frac{k_s}{Bk_g}\right) - \left(\frac{B+1}{2}\right) - \frac{(B-1)}{\left(1 - B\frac{k_g}{k_s}\right)}\right]$$

and

$$B = 1.25\left(\frac{1 - \alpha_D}{\alpha_D}\right)^{10/9}$$

Local contact measurements (Chandran and Chen, 1982) indicated that at near minimum fluidization conditions the top surface of the tube remains covered by a stagnant cap of densely packed particles with very long contact times. The unsteady state component (h_s) would approach zero for this case, whereas heat transfer measurements indicate a small but finite value for the local heat transfer coefficient (h, and in turn h_D). This may be attributed to the effect of fluid flow, as outlined earlier. Since the two-phase theory of fluidization (Davidson and Harrison, 1963) indicates that the dense phase could be considered as an emulsion at the incipiently fluidized state, it is proposed that the component h_f that accounts for the ventilation effect approach the following limits:

$$\lim_{Fo \to 0} h_f = 0$$
$$\lim_{Fo \to \infty} h_f = h_{mf} \tag{9}$$

The ventilation effect is visualized as a secondary process and heat transfer is envisaged to occur from the particles to the fluid by convection. This prompts the use of a weighting factor that depends on the depth of heat penetration. By using a simple relation for the weighting factor that approaches the limits given by Eq. 9, h_f is expressed as

$$h_f = \left[1 - \exp\left(-\frac{x_p}{\bar{d}_p}\right)\right]h_{mf} \tag{10}$$

If x_p is defined as the depth at which the normalized temperature difference $[(T - T_B)/(T_w - T_B)]$ attains a value of 0.01, the use of semi-infinite layer approximation yields

$$x_p/\bar{d}_p \simeq 3.6\sqrt{Fo} \tag{11}$$

Here, the effect of conductivity ratio (k_D/k_g) on the penetration depth is disregarded, for the sake of simplicity.

Some data and correlations for h_{mf} are reported in the literature for vertical tubes. These however cannot be used in Eq. 10, because the fluidization data of Chandran and Chen (1982) indicate packet renewal and lean phase contact to occur at the sides of the tube ($\beta = 90°$) near minimum fluidization conditions. Hence, as a first approximation, the values of the local heat transfer coefficient obtained by Chandran et al. (1980) for the top location ($\beta = 0°$) have been used to derive a curve-fit relation:

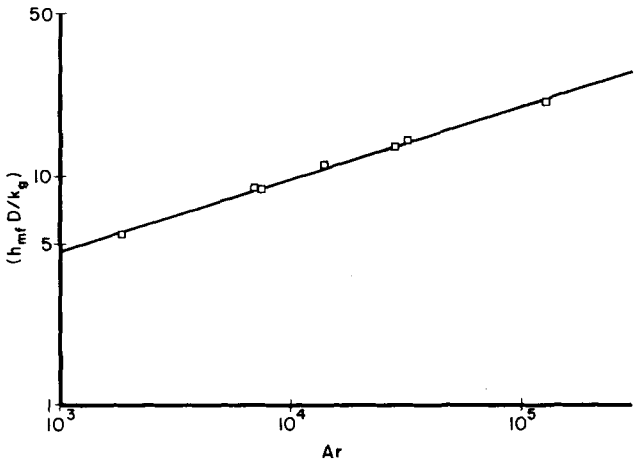

Figure 1. Correlation for heat transfer coefficient at minimum fluidization condition and in the absence of surface renewal.

$$\frac{h_{mf}D}{k_g} = 0.26Ar^{0.31} \tag{12}$$

The data for the top location at minimum fluidization conditions (7 points) and the correlation are shown in Figure 1.

Thus, the effective heat transfer coefficient in the dense phase (h_D) could be estimated by using Eqs. 3, 4, and 10.

Lean-Phase Heat Transfer

Heat transfer during lean-phase contact is hypothesized to occur by fluid convection mechanism. The lean phase is conceptually visualized as a dilute mixture of entrained solid particles in gas. It is stipulated that the heat transfer process between this flowing lean mixture and the tube surface could be considered similar to that of solid-gas mixtures in pneumatic transport.

Data and correlations for heat transfer coefficients have been reported in the literature (Boothroyd, 1971; Depew and Kramer, 1973; Shrayber, 1976) for the flow of gas-solid suspensions in pipes. The equations are in general of the form

$$\frac{h_L}{h_g} = f\left(\frac{G_s}{G_g}, \frac{c_{ps}}{c_{pg}}\right) \tag{13}$$

The quantity G_s/G_g is usually termed solids mass loading ratio.

Depew and Kramer (1973) attribute the improvement in heat transfer to the reduction in the thickness of the viscous sublayer and the increase in the volumetric specific heat of the flow. Shrayber (1976) claims that the higher heat transfer coefficient results primarily from transverse particle migration. The mechanism that causes transverse migration is said to be eddy diffusion in the case of moderate size particles ($\bar{d}_p \sim 30$ to 500 μm and $\rho_s/\rho_g \sim 1{,}000$) and collisions in the case of large particles. It seems that the presence of particles tends to distort the velocity field of the gas stream and affect the flow structure near the wall. It is possible to carry out an analysis if the velocity field and the shear stress at the boundary of gas-solid flow are known. Such treatment, however, becomes elusive for cylinders in crossflow due to the complexity of the problem. There is an obvious need for some basic studies in the area of gas-solid flows. Due to lack of information, a semiempirical approach is adopted here.

For dispersed flow, it would be a reasonable approximation to write the constitutive equations based on a complete mixing model of two-phase flow (Hsu and Graham, 1976). This approach may be applied to gas-solid flow by treating the mixture as a quasi-continuum. The gas flow data of this investigation (Chandran, 1980) indicate that the operating gas velocity for fluidization is not large enough for gas flow in the lean phase to be turbulent. If the lean phase is constituted by closely-sized spherical particles with a large density ratio ($\rho_s/\rho_g \gg 1$), drag force turns out to be the significant force term that influences the motion of the particle (Klinzing, 1981). The momentum equation for the gas phase under steady state conditions then reduces to a form similar to a single fluid momentum equation plus a term due to the resistance force of the particles per unit volume (Boothroyd, 1971). The latter is an interaction term that accounts for the presence of particles in the gas phase. In the present case, the reaction force is primarily due to drag force. Thus the momentum transport equation provides a new similarity parameter to account for particle-gas interaction. For non-turbulent flow of gas in the lean phase, the ratio of drag force to inertia force $\{[3(1-\alpha_L)C_d\rho_g(U_{rg}-U_{rs})^2/4\bar{d}_p]/[\alpha_L\rho_g U_{rg}^2/D]\}$ seems to be the relevant parameter. Consequently, the following relation is proposed for estimating the lean-phase heat transfer coefficient (h_L):

$$\left(\frac{h_L - \alpha_L h_g}{h_g}\right) = f\left[\frac{(1-\alpha_L)}{\alpha_L} C_d \frac{D}{\bar{d}_p}\left(1 - \frac{1}{S}\right)^2\right] \tag{14}$$

The quantity S accounts for slip between the two phases. Based on physical considerations, it is suggested that the magnitude of S is likely to depend upon the value of Archimedes number (Ar). As a first approximation, the slip parameter is expressed in the form

$$S \sim \frac{1}{1 - f_1(Ar)} \tag{15}$$

Ideally, in computing h_L by Eq. 14 for different circumferential positions (β), the local values of h_g for the corresponding locations around the tube should be used. But due to lack of sufficient local information for single phase flow, the value of circumferentially-averaged heat transfer coefficient has to be used instead. Thus, the heat transfer coefficient for gas flow alone (h_g) is estimated from standard correlations for single-phase flow across tubes:

$$\left(\frac{h_g D}{k_g}\right) = b\left(\frac{\rho_g U_{gm} D}{\mu_g}\right)^n (Pr)^{1/3} \tag{16}$$

The constants b and n for single tube configuration have been taken from Holman (1976) and for the case of 10-row bare tube bundle from Zukauskas (1972).

A correlation for $(h_L - \alpha_L h_g)/h_g$ can now be obtained through regression analysis, by using paired curve-fit values from local heat transfer and local fluidization measurements where lean-phase contact dominates.

A satisfactory curve-fit was obtained (multiple correlation coefficient of ~0.7 for 222 data points) with the relation:

$$\left(\frac{h_L - \alpha_L h_g}{h_g}\right) = 0.24\left[\frac{(1-\alpha_L)}{\alpha_L} C_d \frac{D}{\bar{d}_p} Ar^{0.36}\right]^{0.57} \tag{17}$$

Figure 2 indicates the degree of correlation between this equation and the data.

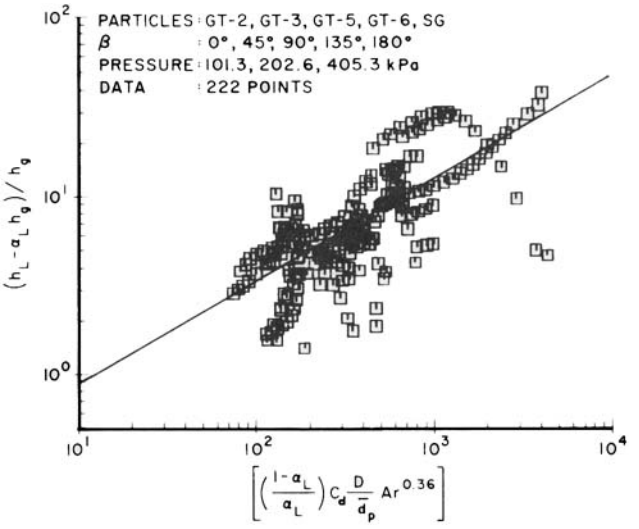

Figure 2. Correlation for effective heat transfer coefficient in the lean phase.

Designation	Mean Size $\bar{d}_p$, μm	Size Range, μm	U_{mf}, m/s Pressure, kPa 101.3	202.6	405.3	U_t, m/s Pressure, kPa 101.3	202.6	405.3
GT-1	125	105–149	0.024			0.83		
GT-2	245	210–297	0.051	0.051	0.050	1.66	1.32	1.07
GT-3	610	500–707	0.280	0.254	0.231	3.91	3.10	2.46
GT-5	950	707–1,190	0.430	0.337	0.267	5.56	4.41	3.37
GT-6	1,580	1,410–1,679	0.801		0.512	9.47		4.74
SG	650	595–707	0.31			4.6		

Material: Soda Lime Glass
Density ρ_s: 2,480 kg/m^3
Specific heat c_{ps}: 753 J/kg·K
Thermal conductivity k_s: 0.89 w/m·K

Design Relation

In summary, the final form of Eq. 2 for the evaluation of the local heat transfer coefficient (h) is:

$$h = f_L\left[\alpha_L + 0.24h_g\left\{\frac{(1-\alpha_L)}{\alpha_L}C_d\frac{D}{\bar{d}_p}Ar^{0.36}\right\}^{0.57}\right] + (1-f_L)\left[2C\sqrt{\frac{k_D C_{pD}}{\pi\bar{\theta}_D}} + \{1-\exp(-3.6\sqrt{Fo})\}h_{mf}\right] \quad (18)$$

The input parameters required are the physical properties of the gas and the solid (ρ_g, k_g, c_{pg}, μ_g, ρ_s, c_{ps}, k_s), the geometric factors ($\bar{d}_p$, D), the fluidization parameters ($\bar{\theta}_D$, f_L, α_D, α_L), and the system variables (U_{sg}, U_{gm}). The values of h_g, C, and h_{mf} are required for using the relation above and are to be calculated from Eqs. 16, 6, and 12, respectively.

Generally, for a given application, all but the fluidization parameters are known. The fluid dynamic information ($\bar{\theta}_D$, f_L, α_D, α_L), however, ought to be determined from independent experiments. Only a few measurements of this type have been reported to date (Ozkaynak and Chen, 1978; Chandran and Chen, 1982). More fluid dynamic experiments need be performed in order to generate general correlations for the fluidization parameters.

COMPARISON OF MODEL PREDICTIONS WITH EXPERIMENTAL DATA

Local Heat Transfer Coefficients

Using curve-fit values of the experimentally determined fluidization parameters $\bar{\theta}_D$, f_L, α_D, and α_L (Chandran and Chen, 1982), it was possible to compute local heat transfer coefficients by the proposed model (denoted as DPLP model hereafter). Comparisons of the predicted local coefficients with those measured experimentally are shown in Figures 3 through 5. The properties of the test particles used in the experiments are given in Table 1.

Figure 3 shows a plot of the local coefficients for three angular positions ($\beta = 0°$, 90°, and 180°) as a function of gas flow rate. The graph indicates the results for GT-5 particles ($\bar{d}_p = 950$ μm) at a system pressure of 202.6 kPa. General agreement is found between the calculated values (points) and the experimental data (curve). It is seen that at low gas flow rates ($U_N < 0.1$), the predicted values tend to be lower than the experimentally measured coefficients; but at higher flow rates, the coefficients show good agreement. In particular, the model successfully predicts the trends exhibited by the experimentally measured local heat transfer coefficients.

Figure 4 presents the results obtained in a 10-row bare tube bundle with SG particles ($\bar{d}_p = 650$ μm) and at atmospheric pressure. It is seen that the model is able to predict the variation in the local heat transfer coefficient with circumferential position reasonably well.

The results plotted in terms of the coordinates (h_{ex}/h_{pr}) and Re are shown in Figure 5. The plot includes both single tube and tube bundle data and covers a wide range of test conditions, as indicated in the figure (546 data points). It is observed that the model is able to successfully predict the variation in the local heat transfer coefficient with circumferential position, gas flow rate, particle size, and system pressure. This result seems to verify the basic mechanisms and their interrelationship as proposed in the phenomenological model. In particular, it appears that the concepts of a dense-phase and a lean-phase transfer mechanism, with each mechanism playing a dominant role at different test conditions, can in fact represent the heat transfer process.

In a previous paper (Chandran and Chen, 1982) it was pointed out that the contributions from and the relative importance of the two transfer mechanisms change appreciably with variations in the test conditions. Herein the effect of system parameters on the individual contributions is examined. Figure 6 indicates the influence of operating pressure on the effective heat transfer coefficients in the dense phase (h_D) and in the lean phase (h_L) for a flow parameter (U_N) value of 0.20. The results obtained at the top of the tube ($\beta = 0°$) indicate that the dense-phase transient conduction mechanism predominates in the case of small particles ($\bar{d}_p = 245$ μm). Both h_D and h_L exhibit increasing trends with pressure and thereby increase the local heat transfer coefficient (h). The h_D and h_L values computed for the side location ($\beta = 90°$) are shown for the case of large particles ($\bar{d}_p = 950$ μm). The dense-phase coefficient exhibits a decreasing trend, whereas the lean-phase coefficient shows a rising characteristic. At atmospheric pressure, the two coefficients are comparable in magnitude with a slightly higher value for h_D. This disposition quickly reverses with an increase in

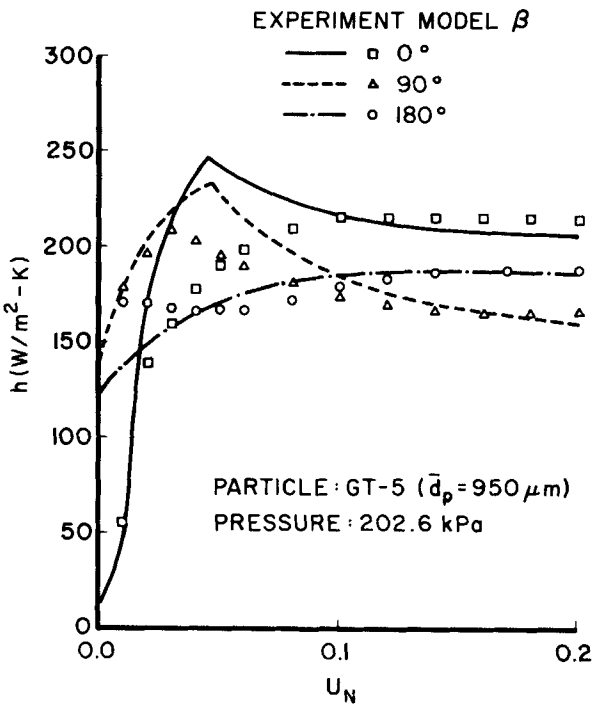

Figure 3. Comparison of model predictions with experimental measurements of local heat transfer coefficient.

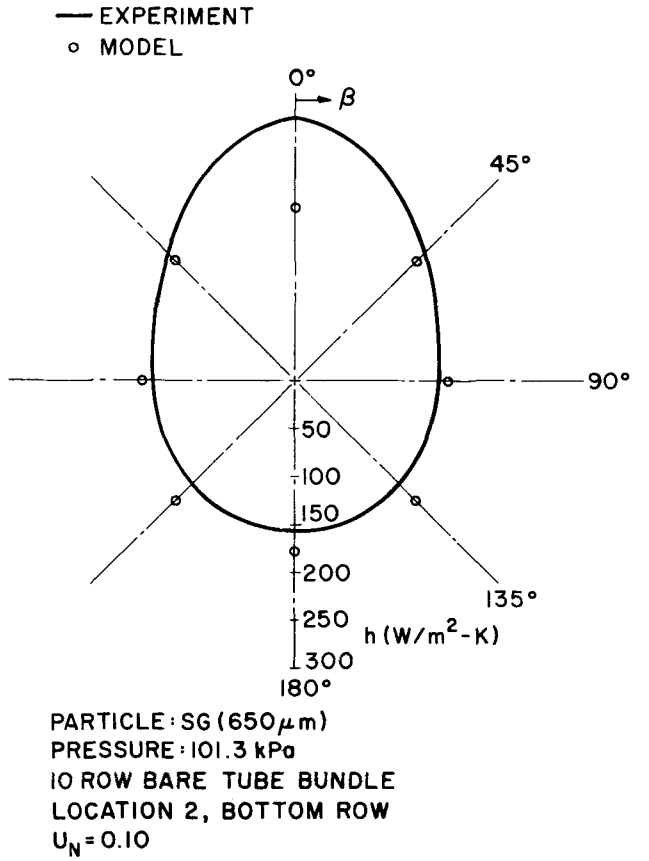

Figure 4. Comparison of model predictions with experimental measurements of local heat transfer coefficient.

pressure, and the value of h_L becomes increasingly greater than that of h_D. Thus the lean-phase convective mechanism provides the basis for the improvement in the local heat transfer coefficient (h) with pressure. Another distinctly different behavior is observed at the bottom of the tube. The data correspond to medium size particles ($\bar{d}_p$ = 610 μm). It is seen that the values of h_D are considerably higher than those of h_L. But the dense-phase coefficient shows little change, while the lean-phase coefficient increases with pressure. The end result is a slight increment in h with pressure. In this manner, the two transfer coefficients (h_D and h_L) change both in magnitude and in their relative importance to provide the variation in the local heat transfer coefficient (h) with test parameters. These observations are in agreement with those reported by Borodulya et al. (1980).

Average Heat Transfer Coefficients

From the local heat transfer coefficients (h) calculated in the

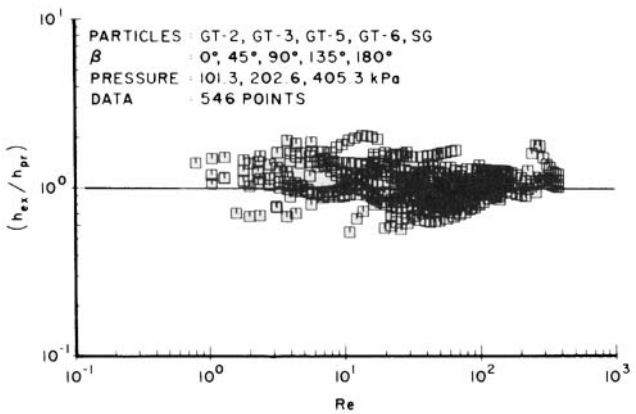

Figure 5. Comparison of experimental data for local heat transfer coefficient with model predictions.

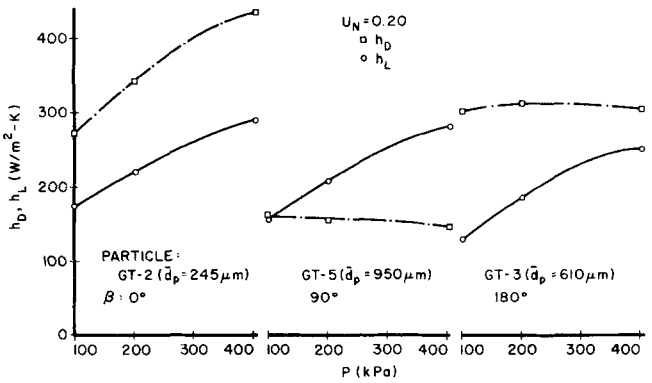

Figure 6. Influence of system pressure on effective heat transfer coefficients in dense and lean phases.

manner outlined in the previous subsection, it was simple to compute the circumferentially averaged heat transfer coefficients ($\bar{h}$). The DPLP model predictions are compared with experimentally determined average coefficients in Figures 7 through 9.

Figure 7 shows a plot of the average heat transfer coefficient versus particle size for a constant flow-rate parameter and at a constant pressure. It is seen that the trend is well predicted and the deviation between calculated and measured coefficients is generally less than 10%.

Using the extrapolated correlation curves presented in Chandran and Chen (1982) for the fluidization parameters ($\bar{\theta}_D, f_L, \alpha_D, \alpha_L$) in a tube bundle, it was possible to calculate the average heat transfer coefficients beyond the range over which actual experimental measurements were obtained. The curve predicted thus for SG particles ($\bar{d}_p$ = 650 μm) at atmospheric pressure is shown in Figure 8. Also included in this figure are points representing experimentally measured $\bar{h}$ obtained with two different instrumented test tubes. These two sets of data were complementary in that the measurements obtained by Chandran et al. (1980) were at low gas flow rates while the measurements of Staub et al. (1978) were at relatively high gas flow rates. It is seen that the model is able to predict the trend of the data reasonably well and shows fair agreement with both sets of data.

Figure 9 presents the data (145 data points) in terms of the coordinates ($\bar{h}_{ex}/\bar{h}_{pr}$) and Re. The plot includes both single tube and tube bundle results and serves to provide an overall evaluation of the model. It is seen that the proposed model is able to make satisfactory predictions despite the wide variation in the test parameters. Also, an examination of Figure 9 in contrast with those (Figures 12–14) presented in Chandran et al. (1980) reveals that the proposed phenomenological model renders vastly improved predictions as compared to the correlations of Vreedenberg, Gelperin et al., and modified Vreedenberg as proposed by Andeen and Glicksman (lit. cit. in Chandran et al., 1980).

Xavier and Davidson (1978) and Xavier et al. (1980) have proposed a model for the average heat transfer coefficient ($\bar{h}$) based on particle-convective and gas-convective contributions. In order

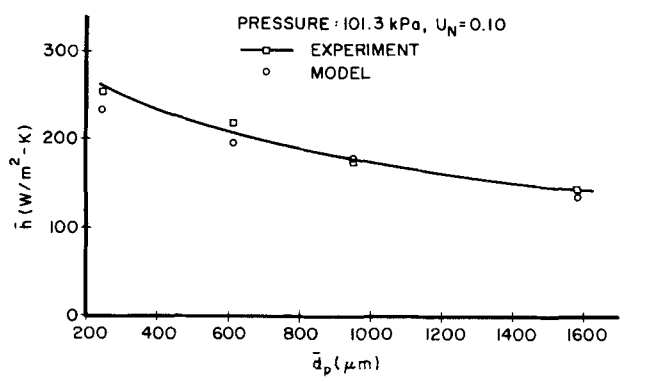

Figure 7. Comparison of model predictions with experimentally-determined values of average heat transfer coefficient.

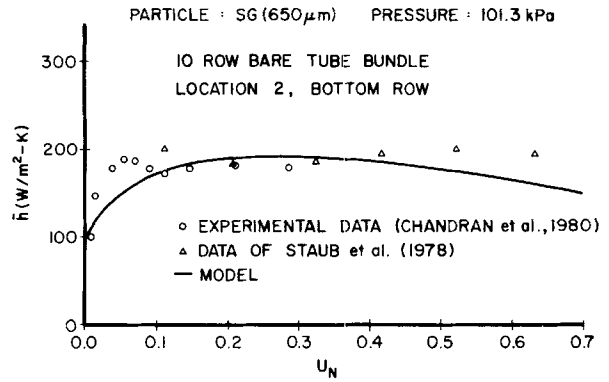

Figure 8. Comparison of model predictions with experimentally-determined values of average heat transfer coefficient.

to compare their model with the DPLP model, a plot similar to Figure 9 was done using the same experimental data (145 points). Comparison of data with their model is shown in Figure 10. Fair agreement between the predictions and the data is observed. From an examination of Figures 9 and 10, however, the DPLP model presented here is seen to be superior.

SUMMARY

With a knowledge of the fluidization characteristics around horizontal tubes, a phenomenological model for the local heat transfer coefficient has been developed based on combined dense phase and lean phase transfer mechanisms. Comparisons with experimental data have indicated that the DPLP model does successfully predict the variation in both local and average heat transfer coefficients with gas flow rate, particle size and system pressure.

There is a tendency for the model to underpredict the heat transfer coefficients at low gas velocities. This discrepancy generally occurs in instances when the dense-phase conduction mechanism prevails. It seems that the deviation probably results from a mismatch in the wall boundary condition. The transient conduction coefficients (h_s) are based on a constant-wall-temperature boundary condition, but the measurements are likely to correspond to a physical condition somewhere between constant heat flux and constant temperature at the wall, due to the use of a heat transfer probe of low thermal capacity. It turns out that the solution for a constant-heat-flux boundary condition is numerically larger than that for a constant-temperature boundary condition and hence an intermediate solution is likely to provide a correction in the right direction. Additional improvement ought to result if the empirical constants in the lean-phase correlation (Eq. 17) are determined from experimental data in the freeboard region of the fluidized bed.

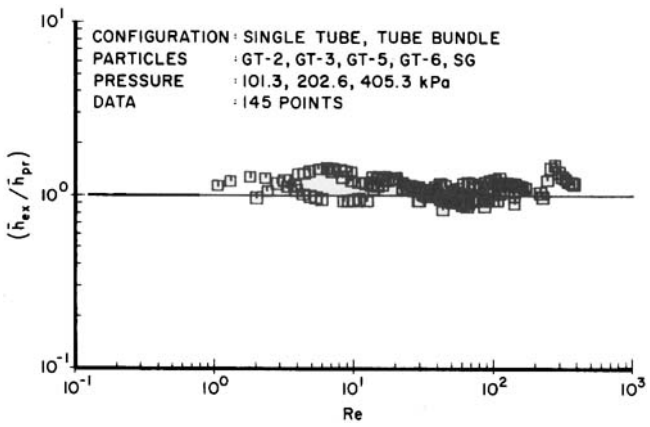

Figure 9. Comparison of experimental data for average heat transfer coefficient with DPLP model predictions.

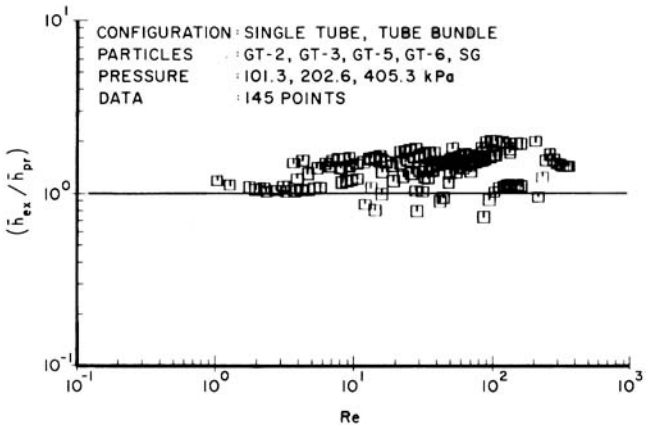

Figure 10. Comparison of experimental data for average heat transfer coefficient with model of Xavier and Davidson (1978) and Xavier et al. (1980).

More experimental investigations with different gas-solid combinations are suggested in order to fully verify the proposed heat transfer model. There is also a need to incorporate the effect of radiation and extend the cold model to hot bed conditions.

ACKNOWLEDGMENT

The authors are grateful for the support of this investigation at Lehigh University by the Corporate Research and Development Center of General Electric Company.

NOTATION

Ar = Archimedes number, $g\bar{d}_p^3\rho_g(\rho_s - \rho_g)/\mu_g^2$
a_1,a_2,a_3 = coefficients in Eq. 6
B = geometric factor, Eq. 8
b = coefficient in Eq. 16
C = effective correction factor, Eq. 4
C_d = particle drag coefficient
C_p = volumetric specific heat
c_p = specific heat
D = tube diameter
$\bar{d}_p$ = mean particle diameter
Fo = time-mean Fourier modulus $(k_D\bar{\theta}_D)/(C_{pD}\bar{d}_p^2)$
$f(\ ),f_1(\ )$ = function of the parameters in parentheses
f_L = fraction of the total time that lean phase is in contact with the tube surface
G = superficial mass velocity
h = local heat transfer coefficient, time-averaged
$\bar{h}$ = average heat transfer coefficient, circumferentially-averaged
h_D = effective heat transfer coefficient in the dense phase
h_f = heat transfer coefficient that accounts for the effect of fluid flow on conduction
h_g = heat transfer coefficient for gas flow alone
h_L = effective heat transfer coefficient in the lean phase
h_{mf} = heat transfer coefficient at minimum fluidization condition and in the absence of surface renewal
h_s = heat transfer coefficient due to surface renewal of a dense medium with stagnant fluid
I = number of dense-phase contacts in the sample time period
k = thermal conductivity
k^o = thermal conductivity in a packed medium with motionless fluid
k' = thermal conductivity due to heat flow through solid-fluid-solid, Eq. 8
n = exponent in Eq. 16
P = absolute pressure

Pr = Prandtl number, $(c_{pg}\mu_g)/k_g$
q = local heat flux
q_D = local heat flux during dense-phase contact
q_L = local heat flux during lean-phase contact
Re = Reynolds number, $(Gd_p)/\mu_g$
S = slip parameter, U_{rg}/U_{rs}
T = temperature
U_{gm} = gas velocity based on minimum flow area
U_{mf} = superficial gas velocity at minimum fluidization condition
U_N = normalized velocity parameter or reduced velocity, $(U_{sg} - U_{mf})/(U_t - U_{mf})$
U_{rg} = real velocity of gas
U_{rs} = real velocity of solid
U_{sg} = superficial gas velocity
U_t = particle terminal or free-fall velocity
w = natural log of conductivity ratio, $\ln(k_D/k_g)$, Eq. 6
x_p = heat penetration depth

Greek Letters

α = void fraction
β = angular position around the circumference of tube, measured from the top of the tube
θ = residence time
$\overline{\theta}_D$ = dense phase root-square-average residence time, Eqs. 5 and A2
μ = dynamic viscosity
ρ = density

Subscripts

B = bed, away from the tube surface
D = dense phase
e = effective value
ex = experimental value
g = gas
L = lean phase
pr = value predicted by model
s = solid particle
w = wall/tube surface

APPENDIX

For constant wall-heat-flux boundary condition, the following form of the equation for the surface renewal component (h_s) is suggested:

$$h_s = \frac{3}{4} C \sqrt{\frac{\pi k_D C_{pD}}{\overline{\theta}_D}} \tag{A1}$$

with

$$\overline{\theta}_D = \left[\sum_{i=1}^{I} \theta_{D_i}^{3/2} \Big/ \sum_{i=1}^{I} \theta_{D_i} \right]^2 \tag{A2}$$

The effective correction factor C for this case ought to be determined by comparison with a numerical solution for constant wall-heat-flux boundary condition.

LITERATURE CITED

Adams, R. L., and J. R. Welty, "A Gas Convection Model of Heat Transfer in Large Particle Fluidized Beds," *AIChE J.*, **25**, 395 (1979).

Ainshtein, V. G., and N. I. Gelperin, "Heat Transfer between a Fluidized Bed and a Surface," *Int. Chem. Eng.*, **6**(1), 67 (1966).

Antonishin, N. V., M. A. Geller, and A. L. Parnas, "Hyperbolic Equation of Heat Conduction for Dispersed Systems," *J. Eng. Phys.*, **26**(3), 353 (1974).

Baskakov, A. P., "The Mechanism of Heat Transfer between a Fluidized Bed and a Surface," *Int. Chem. Eng.*, **4**(2), 320 (1964).

Baskakov, A. P., and V. M. Suprun, "Determination of the Convective Component of the Heat Transfer Coefficient to a Gas in a Fluidized Bed," *Int. Chem. Eng.*, **12**(2), 324 (1972).

Baskakov, A. P., et al., "Heat Transfer to Objects Immersed in Fluidized Beds," *Powder Technol.*, **8**, 273 (1973).

Bauer, R., and E. U. Schlunder, "Effective Radial Thermal Conductivity of Packings in Gas Flow. II: Thermal Conductivity of the Packing Fraction without Gas Flow," *Int. Chem. Eng.*, **18**(2), 189 (1978).

Berg, B. V., and A. P. Baskakov, "Investigation of Local Heat Transfer between a Fixed Horizontal Cylinder and a Fluidized Bed," *Int. Chem. Eng.*, **14**(3), 440 (1974).

Bock, H. J., and O. Molerus, "Influence of Hydrodynamics on Heat Transfer in Fluidized Beds," *Fluidization*, J. R. Grace and J. M. Matsen, Eds., Plenum Press, New York, 217 (1980).

Boothroyd, R. G., *Flowing Gas-Solids Suspensions*, Chapman and Hall Ltd., London (1971).

Borodulya, V. A., V. G. Ganzha, and A. I. Podberezsky, "Heat Transfer in a Fluidized Bed at High Pressure," *Fluidization*, J. R. Grace and J. M. Matsen, Eds., Plenum Press, New York, 201 (1980).

Botterill, J. S. M., and J. R. Williams, "The Mechanism of Heat Transfer to Gas-Fluidized Beds," *Trans. Inst. Chem. Eng.*, **41**, 217 (1963).

Botterill, J. S. M., and M. H. D. Butt, "Achieving High Heat Transfer Rates in Fluidized Beds," *Br. Chem. Eng.*, **13**(7), 1,000 (1968).

Botterill, J. S. M., and M. Desai, "Limiting Factors in Gas-Fluidized Bed Heat Transfer," *Powder Technol.*, **6**(4), 231 (1972).

Botterill, J. S. M., Y. Teoman, and K. R. Yuregir, "Temperature Effects on the Heat Transfer Behavior of Gas-Fluidized Beds," *AIChE Symp. Ser.*, **77**(208) 330 (1981).

Canada, G. S., and M. H. McLaughlin, "Large Particle Fluidization and Heat Transfer at High Pressures," *AIChE Symp. Ser.*, **74**(176), 27 (1978).

Catipovic, N. M., et al., "A Model for Heat Transfer to Horizontal Tubes Immersed in a Fluidized Bed of Large Particles," *Fluidization*, J. R. Grace and J. M. Matsen, Eds., Plenum Press, New York, 225 (1980).

Catipovic, N. M., et al., "Experimental Validation of the Adams-Welty Model for Heat Transfer in Large-Particle Fluidized Beds," *AIChE J.*, **28**(5), 714 (1982).

Chandran, R., J. C. Chen, and F. W. Staub, "Local Heat Transfer Coefficients around Horizontal Tubes in Fluidized Beds," *J. Heat Transfer (Trans. ASME)*, **102**, 152 (1980).

Chandran, R., "Local Heat Transfer and Fluidization Dynamics around Horizontal Tubes in Fluidized Beds," PhD Dissertation, Lehigh Univ., Bethlehem, PA (1980).

Chandran, R., and J. C. Chen, "Bed-Surface Contact Dynamics for Horizontal Tubes in Fluidized Beds," *AIChE J.*, **28**(6), 907 (1982).

———, "Influence of the Wall on Transient Conduction into Packed Media," *AIChE J.*, **31** (Jan., 1985).

Chen, J. C., "Heat Transfer to Tubes in Fluidized Beds," *ASME Paper 76-HT-75*, ASME-AIChE Heat Trans. Conf., St. Louis, MO (1976).

Davidson, J. F., and D. Harrison, *Fluidized Particles*, Cambridge Univ. Press, New York (1963).

Denloye, A. O. O., and J. S. M. Botterill, "Bed-to-Surface Heat Transfer in a Fluidized Bed of Large Particles," *Powder Technol.*, **19**(2), 197 (1978).

Depew, C. A., and T. J. Kramer, "Heat Transfer to Flowing Gas-Solid Mixtures," *Adv. Heat Transfer*, **9**, 113 (1973).

Gabor, J. D., "Wall-to-Bed Heat Transfer in Fluidized and Packed Beds," *Chem. Eng. Prog. Symp. Ser.*, **66**(105), 76 (1970).

Gelperin, N. I., V. G. Ainshtein, and A. V. Zaikovskii, "Variation of Heat Transfer Intensity Around the Perimeter of a Horizontal Tube in a Fluidized Bed," *J. Eng. Phy.*, **10**(6), 473 (1966).

Gelperin, N. I., and V. G. Einstein, "Heat Transfer in Fluidized Beds," *Fluidization*, J. F. Davidson, and D. Harrison, Eds., Academic Press, London, 471 (1971).

Glicksman, L. R., and N. A. Decker, "Design Relationships for Predicting Heat Transfer to Tube Bundles in Fluidized Bed Combustors," *Proc. 6th Int. Conf. on Fluidized Bed Combustion*, **III**, U.S. Dept. of Energy, Washington, D.C., 1,152 (1980).

Grewal, N. S., and S. C. Saxena, "Heat Transfer between a Horizontal Tube and a Gas-Solid Fluidized Bed," *Int. J. Heat Mass Transfer*, **23**(11), 1,505 (1980).

Grewal, N. S., and S. C. Saxena, "Maximum Heat Transfer Coefficient between a Horizontal Tube and a Gas-Solid Fluidized Bed," *Ind. Eng. Chem. Proc. Des. Dev.*, **20**(1), 108 (1981).

Gutfinger, C., and N. Abuaf, "Heat Transfer in Fluidized Beds," *Adv. Heat Transfer*, **10**, 167 (1974).

Holman, J. P. *Heat Transfer*, 4th Ed., McGraw-Hill, New York, 216 (1976).

Hsu, Y. Y., and R. W. Graham, *Transport Processes in Boiling and Two-Phase Systems*, Hemisphere Pub. Corp., Washington (1976).

Klinzing, G. E., *Gas-Solid Transport*, McGraw-Hill, New York (1981).
Koppel, L. B., R. D. Patel, and J. T. Holmes, "IV: Wall to Fluidized Bed Heat Transfer Coefficients," *AIChE J.*, **16**, 464 (1970).
Krause, W. B., and A. R. Peters, "Heat Transfer Mechanisms Near Horizontal Heat Exchange Tubes in an Air-Fluidized Bed of Uniformly Sized Glass Particles," ASME Paper 79-HT-88, Joint ASME/AIChE 18th Natl Heat Transfer Conf., San Diego (1979).
Kubie, J., and J. Broughton, "A Model of Heat Transfer in Gas-Fluidized Beds," *Int. J. Heat Mass Trans.*, **18**, 289 (1975).
Kunii, D., and J. M. Smith, "Heat Transfer Characteristics of Porous Rocks," *AIChE J.*, **6**(1), 71 (1960).
Kunii, D., and S. Yagi, "Studies on Heat Transfer Near Wall Surface in Packed Beds," *AIChE J.*, **6**(1), 97 (1960).
Mickley, H. S., and D. F. Fairbanks, "Mechanism of Heat Transfer to Fluidized Beds," *AIChE J.*, **1**, 374 (1955).
Mickley, H. S., D. F. Fairbanks, and R. D. Hawthorn, "The Relation Between the Transfer Coefficient and Thermal Fluctuations in Fluidized-Bed Heat Transfer," *Chem. Eng. Prog. Symp. Ser.*, **57**(32), 51 (1961).
Ozkaynak, T. F., and J. C. Chen, "Average Residence Times of Emulsion and Void Phases at the Surface of Heat Transfer Tubes in Fluidized Beds," *AIChE Symp. Ser.*, **74**(174), 334 (1978).
———, "Evaluation of the Emulsion Phase Residence Times in Fluidized Beds and Its use in Heat Transfer Models," *AIChE J.*, **26**(4), 544 (1980).
Saxena, S. C., et al., "Heat Transfer between a Gas-Fluidized Bed and Immersed Tubes," *Adv. Heat Transfer*, **14**, 149 (1978).
Saxena, S. C., and J. D. Gabor, "Mechanisms of Heat Transfer between a Surface and a Gas-Fluidized Bed for Combustor Application," *Prog. Energy Combust. Sci.*, **7**(2), 73 (1981).
Selzer, V. W., and W. J. Thomson, "Fluidized Bed Heat Transfer—The Packet Theory Revisited," *AIChE Symp. Ser.*, **73**(161), 29 (1977).
Shrayber, A. A., "Turbulent Heat Transfer in Pipe Flows of Gas-Conveyed Solids," *Heat Transfer—Sov. Res.*, **8**(3), 60 (1976).
Staub, F. W., et al., "Two-Phase Flow and Heat Transfer in Fluidized Beds," Final Technical Report, SRD-78-103, Thermal Branch, General Electric Company, Schenectady, NY (1978).
Staub, F. W., "Solids Circulation in Turbulent Fluidized Beds and Heat Transfer to Immersed Tube Banks," *J. Heat Transfer, Trans. ASME*, **101**, 391 (1979).
Toor, H. L., and J. M. Marchello, "Film-Penetration Model for Mass and Heat Transfer," *AIChE J.*, **4**(1), 97 (1958).
van Heerden, C., A. P. P. Nobel, and D. W. van Krevelen, "Mechanism of Heat Transfer in Fluidized Beds," *Ind. Eng. Chem.* **45**(6), 1,237 (1953).
Xavier, A. M., and J. F. Davidson, "Heat Transfer to Surfaces Immersed in Fluidized Beds, Particularly Tube Arrays," *Fluidization*, J. F. Davidson and D. L. Keairns, Eds., Cambridge Univ. Press, London, 333 (1978).
Xavier, A. M., et al., "Surface-Bed Heat Transfer in a Fluidized Bed at High Pressure," *Fluidization*, J. R. Grace and J. M. Matsen, Eds., Plenum Press, New York, 209 (1980).
Yoshida, K., D. Kunii, and D. Levenspiel, "Heat Transfer Mechanisms between Wall Surface and Fluidized Bed," *Int. J. Heat Mass Trans.*, **12**, 529 (1969).
Zabrodsky, S. S., *Hydrodynamics and Heat Transfer in Fluidized Beds*, MIT Press, Cambridge, MA (1966).
Zabrodsky, S. S., N. V. Antonishin, and A. L. Parnas, "On Fluidized Bed-to-Surface Heat Transfer," *Can. J. Chem. Eng.*, **54**, 52 (1976).
Zabrodsky, S. S., et al., "Heat Transfer in a Large-Particle Fluidized Bed with Immersed In-Line and Staggered Bundles of Horizontal Smooth Tubes," *Int. J. Heat Mass Transfer*, **24**(4), 571 (1981).
Ziegler, E. N., and W. T. Brazelton, "Mechanism of Heat Transfer to a Fixed Surface in a Fluidized Bed," *Ind. Eng. Chem. Fund.*, 3(2), 94 (1964).
Ziegler, E. N., L. B. Koppel, and W. T. Brazelton, "Effects of Solid Thermal Properties on Heat Transfer to Gas Fluidized Beds," *Ind. Eng. Chem. Fund.*, 3(4), 324 (1964).
Zukauskas, A., "Heat Transfer from Tubes in Crossflow," *Adv. Heat Transfer*, **8**, 93 (1972).

Manuscript received March 11, 1982; revision received November 28, 1983, and accepted December 6.

A Generalized Model for Predicting Equilibrium Conditions for Gas Hydrates

A modification of van der Waals and Platteeuw's (1959) hydrate equilibrium model which incorporates the effect of spherical asymmetry is developed. A corresponding states correlation is used to predict the deviation of Langmuir constants from ideal values. In this model the Kihara parameters obtained from hydrate equilibrium data agree well with those obtained from virial coefficient data.

V. T. JOHN
K. D. PAPADOPOULOS
Department of Chemical Engineering
Columbia University in the City of New York
New York, NY 10027

and G. D. HOLDER
Chemical and Petroleum Engineering
Department
University of Pittsburgh
Pittsburgh, PA 15261

SCOPE

Gas hydrates are crystalline solids in which water forms a hydrogen bonded lattice with large interstitial vacancies called cavities. These cavities must be partially occupied by small gas molecules such as methane, nitrogen, or propane. Although some of the cavities will always be empty, the water lattice cannot form in the absence of gas; only through the physical interaction between the encaged gas molecules and the water lattice is the hydrate structure stabilized. In recent years much effort has been devoted to modeling the conditions at which hydrates will form.

The prediction of phase equilibria in gas hydrate forming

V. T. John and K. D. Papadopoulos are presently with the Department of Chemical Engineering, Tulane University, New Orleans, LA 70118